FLUORINATION EFFECT ON THE CONFORMATIONAL PROPERTIES OF ALKANES

Wenjian Xu

Thesis Prepared for the Degree of

MASTER OF SCIENCE

UNIVERSITY OF NORTH TEXAS

May 2002

APPROVED:

David Wiedenfeld, Major Professor
Robert Desiderato, Committee Member
Ruthanne Thomas, Chair of the Department of Chemistry
C. Neal Tate, Dean of the Robert B. Toulouse School of Graduate Studies

Xu, Wenjian, Fluorination Effect on the Conformational Properties of Alkanes. Master of Science (Chemistry), May 2002, 47 pp., 13 tables, 39 references.

A Series of fluorophores of the general formular $Pyr(CF_2)_nPyr$ and $Pyr(CF_2)_{n-1}CF_3$ has been synthesized. Copper catalyzed coupling of 1-bromopyrene and the corresponding mono and di-iodoperfluoroalkanes were used in most cases. For the n=3 dimer, a novel 1,ω-perfluoroalkylation of pyrene via bis-decarboxylation of hexafluorogultaric acid was utilized. These compounds, along with suitable hydrocarbon analogs, are being used to study the flexibility of fluorocarbon chains using emission and NMR spectrosopies. We have found that the excimer formation for the fluorinated pyrene monomers is highly dependent on concentration and is less efficient than for pyene. Excimer formation for the fluorinated pyrene dimers is much more efficient than for the fluorocarbon monomers and is only slightly concentraion dependent. Steady-state emission spectra indicate hydrocarbon dimers-models form excimers more efficiently than the fluorinated dimers suggesting the fluorinated chains are stiffer than the hydrocarbons; we conducted the temperature-dependent studies and quantified the conformational difference.

ACKNOWLEDGMENTS

We thank the Robert A. Welch Foundation (Grant B-1415) and the University Of North Texas Research Office for Financial support.

TABLE OF CONTENTS

LIST OF TABLES

Table Page

1. INTRODUCTION

The use of fluorocarbon materials as high-temperature resistant lubricants [1] and insulators [2] highlight the importance of these molecules. These properties of fluorocarbons are thought to be due in part to the rotational barrier of the C-C bonds [3]. Fluorine, being the most electronegative element and among the smallest elements, forms the strongest single bond to carbon encountered in carbon chemistry. This strong covalent bond is accompanied by weak intermolecular forces in perfluorocarbons, as expected from the high ionization potential for fluorine and the low polarity. Aliphatic carbon-carbon bonds are usually strengthened by fluorination and the carbon-fluorine bond lengths decrease progressively with accumulation of fluorines.

The goal of this research program was to study repulsive interactions in terms of the flexibility of perfluoroalkyl chains using temperature dependence steady-state and time-resolved emission spectroscopy. In this project, I synthesized part of the molecules needed for this study and did the preliminary temperature dependence steady-state spectroscopy study.

1.1 Backgrounds of Conformational Study on Hydrocarbons and Fluorocarbons

Aside from the existence of biphenyl isomerism recognized [4] in 1926, the first suggestion of the importance of conformation (i.e., rotational arrangement) on reactivity

in acyclic compounds came characteristically, in a paper by Bo?seken [5] on the reaction of the diastereoisomeric 2,3-butanediols with acetone and on their effect on the conductivity of boric acid. The first suggestion that rotation about single bonds (other than biphenyl bonds) was not free came two years later in a paper [6] on the difference of the dipole moments of the stilbene dichlorides. This conclusion was supported by several other investigations of physical properties in the early 1930's [7], which in turn led to speculation about the energy barrier to rotation about carbon-carbon single bonds.

The early work culminated in 1936 in the important suggestion by Kemp and Pitzer [8] that there is a barrier to rotation in ethane of approximately 3 kcal/mole, an assumption which made possible reconciliation of the experimental data on the heat capacity and entropy of ethane [9] with calculations based on statistical mechanics. The establishment of the ethane barrier probably marks the highlight of the history of conformational analysis in acyclic systems. In ethane (1), the transformation of a S_3 to a C_3 symmetry axis in attaining the eclipse geometry induces a quadrupole polarization of the density in the carbon-carbon bond, causing it to lengthen. This lengthening leads to a decrease in magnitude of the attractive interaction of each carbon nucleus for the electronic charge basin of the other carbon atom and this is thought to be the origin of the barrier.

Van der Waals [10] suggested that the potential energy function for the interaction between two rare gas atoms had a short-range repulsive term arising from electron-electron repulsions and incompletely screened nuclei. And a long-range attractive term arosed mainly from London dispersive forces. The energy of molecules containing permanent charges or dipole moments depends on interaction of these charges

or dipoles with other charges or dipoles in the same molecule or in surrounding molecules. So, the effect of electrostatic interactions depends on the conformation of the molecules as well as on the medium.

n-butane (2) has two stable conformations, called "conformational isomers" or sometimes "conformers" [11] .

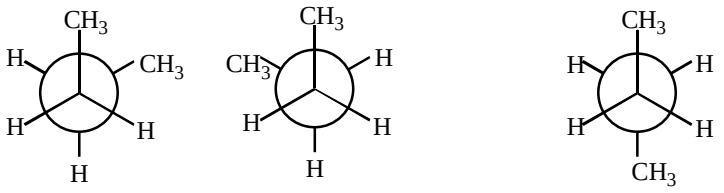

gauche butanes anti butane

Figure 1. Newman projections of gauche and anti butane

The Newman projections of these forms are shown in figure 1. The "gauche" or "skew" isomer is the less stable isomer. The "anti" or "trans" isomer is the more stable isomer. In butane, the gauche and anti forms differ in potential energy by 0.8 kcal/mole, with a barrier height of 3.3-3.6 kcal/mole.

The energy of rotation of atom A and atom B attached on the same framework is composed of three terms to their individual orientation ? :

$$E(?_A,?_B)=E_A(?_A)+E_B(?_B)+E_{AB}(?_A?_B) \qquad 1$$

E_A and E_B is the interaction of the rotors A and B with the framework and E_{AB} is the through space interaction between A and B.

In 1948, Pace and Aston [12] reported their investigation on perfluoroethane motivated by the discovery of barriers in 1,1,1- trifluoroethane (3) and 1,1,1-trichloroethane (4) of the order of 3000 calories per mole, which raises the question of whether the restricted rotation is uniquely a function of the number of hydrogen atoms. By assuming a C-F bond distance of 1.35Å and C-C bond 1.45Å, and the CF_3 group was assumed to be tetrahedral, they calculated the entropy due to translation and external rotation from:

$$S_{t+r} = 4.575(3/2 \log M + 4\log T + 1/2 \log I_x I_y I_z - \log 6) + 265.289 \qquad 2$$

The entropy contribution for the degree of freedom corresponding to the free rotation of the CF_3 was obtained from:

$$S_f = 4.575\ (1/2 \log T + \tfrac{1}{2} \log I_{red}.10^{-40} - \log n) - 1.540\ (n=3 \text{ was used}) \qquad 3$$

Because of the presence of restricted rotation, the contribution S_f was reduced by an amount of $(S_f - S)$ as given by Pitzer's tables [13].

The entropy of the gas has been calculated from a frequency assignment based on the infrared spectrum of the gas and liquid. A potential barrier of 4.35 kcal/mole hindering the mutual rotation of the CF_3 groups in hexafluoroethane gives the best agreement between the calculated and calorimetric entropy. That a barrier exists is indicated by the appearance of only seven lines in the Raman spectrum. If the rotation were free, it should result in more lines in the Raman spectrum.

In 1983, Ted Schaefer, et al [14] reported temperature dependent ^{19}F NMR studies on 2,6-difluoroisopropyl benzene (5). They found that the fluorinated substituents caused obvious increase in the barrier to rotation.

In the spectroscopy study of 1,1-difluoro-1,2,2-trichloroethane (6), it was found that in both the gas phase and liquid phase, the trans conformer was more stable by 330 ?70 and 320 ? 90 cal/mol.

The fluorine atom is smaller than carbon, the van der waals radius for fluorine is more than 20% bigger than for hydrogen, so steric interactions between adjacent fluorines occur in perfluoroalkyl chains. The repulsive interactions between fluorines inhibit free rotation about the backbone carbon-carbon bonds. This property of fluorocarbons is of active research interest and motivated this work.

1.2 Background of Conformational Studies on Pyrene Excimers

Birks defines that an excimer is a dimer which is associated in the electronic excited state and which is dissociative in its ground state [15]. . The formation of a pyrene excimer requires encounter of an electronically excited pyrene with a second pyrene in its ground state. According to this definition, the two pyrenes must be far enough away, so that the incident radiation can cause "localized excitation". These locally excited molecules can cause "monomer" emission. The observation of excimer emission indicates that diffusive encounters between pyrenes have occurred.

There are instances that excimer emission is observed although there is no evidence that the pyrenes (**7**) are separated in the ground state. These excited species are sometimes referred to as "static excimers" while those obeying Birks' defination are

termed as "dynamic excimers". Under normal conditions the distinction between static and dynamic excimers is that one can observe in time-resolved experiments the growth of dynamic excimers while that of static excimers cannot be observed. The associated pyrenes, as distinct from the pyrene excimers, are sufficiently close to exhibit perturbed absorption and excitation spectra.

Fluorescence measurements can be broadly classified into two types of measurements, steady-state and time-resolved [16]. Steady-state measurements are those performed with constant illumination and observation. This is the most common type of measurement. The sample is illuminated with a continuous beam of light, and the intensity or emission spectrum is recorded. Because of the nanosecond timescale of fluorescence, most measurements are steady-state measurements. When the sample is first exposed to light, a steady state is reached almost immediately.

The second type, time-resolved measurements, is used for measuring intensity decays. For these measurements, the sample is exposed to a pulse of light, where the pulse width is typically shorter than the decay time of the sample. This intensity decay is recorded with a high-speed detection system that permits the intensity or anisotropy to be measured on the nanosecond timescale.

It is important to understand that there exists a rather simple relationship between steady-state and time-resolved measurements. The steady-state observation is simply an average of the time-resolved phenomena over the intensity decay of the sample. For instance, consider a fluorophore which displays a single decay time (t) and a single rotational correlation time (?). The intensity and anisotropy decays are given by

$$I(t) = I_0 e^{-t/t} \qquad 4$$

$$r(t) = r_0 e^{-t/?} \qquad 5$$

where I_0 and r_0 are, respectively, the intensities and anisotropies at t = 0, immediately following the excitation pulse.

Equations 4 and 5 can be used to illustrate how the decay time determines what can be observed using fluorescence. The steady-state anisotropy (r) is given by the average of r(t) weighted by I(t):

$$r = \frac{\int_0^{?} r(t)I(t)dt}{\int_0^{?} I(t)dt} \qquad 6$$

In this equation the denominator is present to normalize the anisotropy to be independent of total intensity. In the numerator the anisotropy at any time t contributes to the steady-state anisotropy according to the intensity at time t.

Perhaps a simpler example is how the steady-state intensity I_{ss} is related to the decay time. The steady-state intensity is given by

$$I_{ss} = I_0 \, t \qquad 7$$

The value of I_0 can be considered to be a parameter which depends on the fluorophore concentration and a number of instrumental parameters. Hence, in molecular terms, the steady-state intensity is proportional to the lifetime.

Förster and coworkers [17] first recognized the role of the association of excited molecules as the cause of a change in the fluorescence spectrum with concentration in the case of pyrene and some of its derivatives. In 1964, Stevens and Ban [18] proposed a sandwich configuration of the excimer resulting from the mutual approach of the two components with their molecular planes parallel.

The electronic state of a symmetrical singlet excimer could obviously be described by a resonance hybrid with uniform distribution of the excitation energy over both components:

P*P (ER1) ? PP* (ER2) 8

It is therefore assumed [19] that the stability of the pyrene excimer was due to excitation resonance between the two configurations in formula ER1 and ER2. States with even higher energies have also been considered [20] . A second hypothesis [21] for the state of the excimer was interpreted as a charge-transfer state:

P^+P^- (CR1) ? P^-P^+ (CR2) 9

According to this hypothesis, the energy of the excimer should depend on the difference between the ionization potential and the electron affinity of the monomer.

Either the neutral or the ionic configuration may be predominating depending on the particular case. Quantum chemical calculations on excimers of pyrene were performed by Murrell and Tanaka by the semi-empirical PPP method [22]. These calculations showed that with acceptable values of the parameters involved, and particularly of the distance between the two molecules within the excimer, the position of the excimer band can be reproduced only if both excitation and charge resonance are

taken into account. These correspond to a conclusion that equation **10** is a general form of the excimer state[17]:

$$P^*P \;?\; PP^* \;?\; P^+P^- \;?\; P^-P^+ \qquad 10$$

(ER1) (ER2) (CR1) (CR2)

Besides the PPP method, simpler and less conventional semi-empirical methods have also been use, several of them based on orbitals extending over both components of the excimer [23]. Most of these calculations gave only the excited energy of the excimer as a function of its geometrical configuration. The latter itself and particularly the equilibrium distance between the planes of the two excimers compounds, could be deduced from the agreement of calculated and experimental values for the position of the excimer band. Values between 3.0 and 3.4Å were obtained in every case studied.

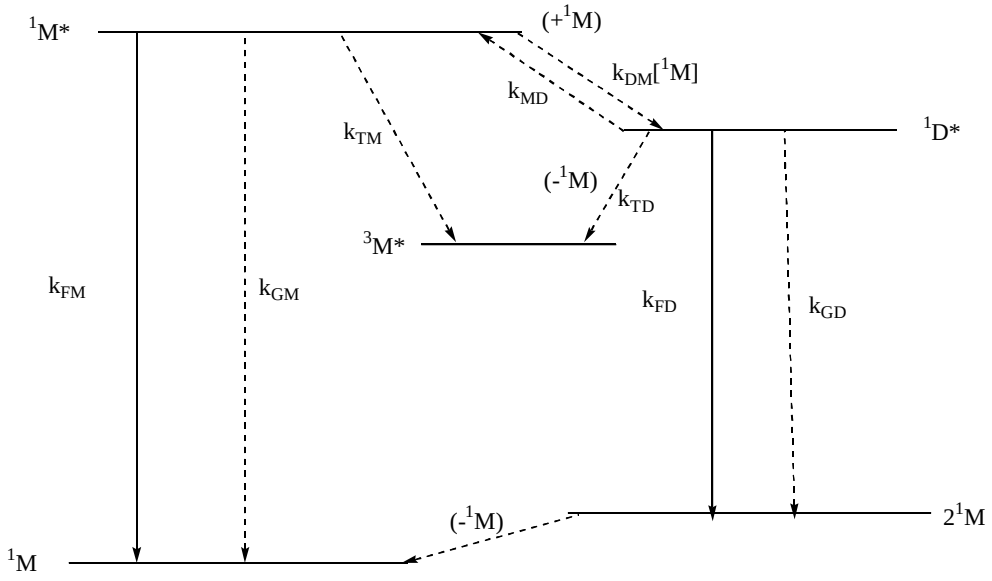

Figure 2. Rate process in monomer/excimer system. Solid lines indicate radiative processes; broken lines indicate radiationless processes.

In the steady-state, the emission of the excimer is obtained after excitation at absorption maxima of the species. The steady-state emission spectra provide two parameters, the ratio I_E/I_M and $?_E$. I_E is the intensity of the excimer emission. I_M is the intensity of the monomer emission. $?_E$ is the wavelength of the maximum of the excimer emission. The Figure 2 represents the excimer formation via Birks' mechanism. k_{FM} is the fluorescence rate of $^1M^*$ state and k_{FD} is the fluorescence rate of the $^1D^*$ state. k_{GM} and k_{GD} are the conversion rates to the ground state from $^1M^*$ and D* state. k_{TM} and k_{TD} are the respective intersystem crossing rates; k_{MD} is the dissociation to $^1M^*$ and the ^1M states of $^1D^*$ while $k_{DM}[^1M^*]$ is the rate of formation of $^1D^*$ from the $^1M^*$ and the ^1M states.

1.3 Conformational Study on Perfluoroalkane Chains Using Pyrene Excimer Emission

Bending and folding motions of hydrocarbon chains are fundamental to many processes in nature. Chain dynamics must first be analyzed to understand the factors controlling them. For this and other reasons, the conformational interconversions of long chains have been studied in detail both experimentally and theoretically. One germane characteristic of chains is their average end-to-end separation, which is a function of temperature, solvent type, the length of the chain, and the rate of conformational change (often referred to as dynamic flexibility) [24]. Long chains possess Gaussian distributions of end-to-end distance; short chains have narrower and distorted end-to-end distributions due to locally hindered motions and excluded-volume effects[25].

Chain dynamics of head-to-tail encounters can be followed by measuring the rate at which a,? -disubstituted chains form intramolecular excimers. This phenomenon was first observed by Hirayama for 1,3-diphenylpropane, which exhibits monolumophoric fluorescence at $?_{max}$ 285 nm and unstructured excimer emission at $?_{max}$ 335nm. Since a ground-state benzene dimmer "complex" is dissociative and the conformation necessary for the two phenyl groups to achieve facial overlap is high in energy, excimer formation occurs sequentially with phenyl excitation followed by chain cyclization. This sequence has been confirmed by analyses of the monomer and excimer emission waveforms of the 1,3-diarylpropanes.

Since Hirayama's [26] initial work with phenyl, the pyrenyl lumophore has been used more widely to study intramolecular chain cyclizations. It possesses a much longer singlet lifetime than phenyl (up to 450 ns va ca. 20 ns), much higher molar extinction

coefficients, a higher fluorescence yield, and well-separated monomer and excimer emissions.

The experimental and fluorescence spectra study of a,? -di-(1-pyrenyl)alkanes $Py(CH_2)_nPy$ (8) with n=2 to 16 and 22 was carried out by K. A. Zachariasse [27] and Perico[28]. According to Zachariasse's, nearly all of the compounds in his experiments form an intramolecular excimer when measured in a $1*10^{-5}$ M solution in methylcyclohexane at room temperature. The intensity ratio of the excimer and monomer fluorescence appeared as a function of chain length, which strongly resembled the dependence of the yields of organic ring closure reactions on ring size. Distortion from the optimal intramolecular sandwich configuration of the pyrene moeties was reflected in a blue shift of the maximum of the excimer emission.

In Zachariasse's subsequent study, the fluorescence response functions of 1,3-di(2-pyrenyl)propane (**9**) in methylcyclohexane can be fitted with two exponentials having the same decay parameters for the excimer and the monomer. This is in contrast to what had

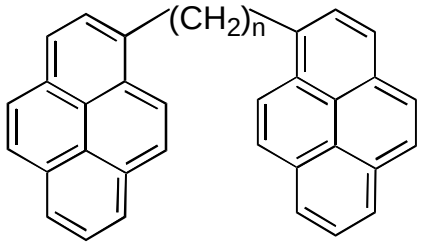

(10)

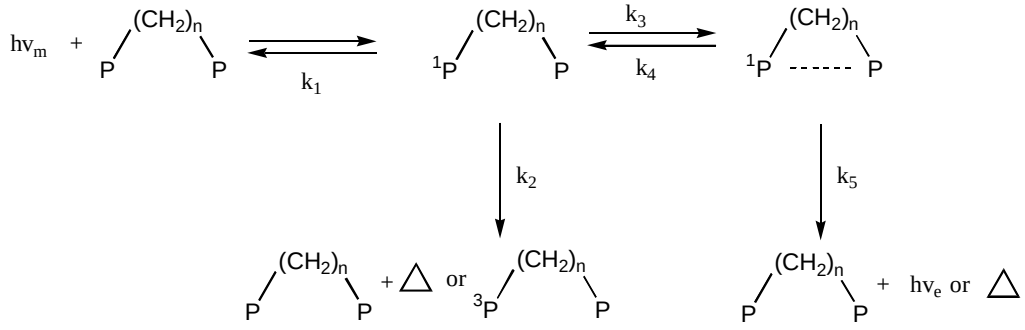

Figure 3. Standard mechanism for intramolecular quenching of Pyr$(CH_2)_n$Pyr in nonpolar solvent.

been observed with 1,3-di(1-pyrenyl)propane (**10**) where three exponentials are required. This meant that conformer of the propane chain act as a single kinetically uniform group in forming excimers. The kinetics scheme applicable to intermolecular excimer formation can also be utilized in the intramolecular case.

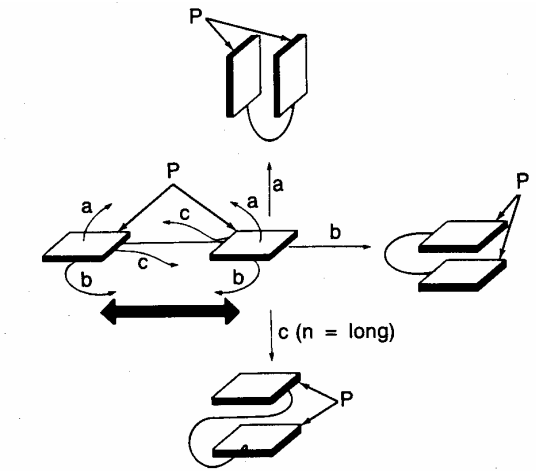

Figure 4. Representation of some possible PnP motions leading to an intramolecular excimer geometry assuming initially extended and planar conformations.

The dynamic flexibility of hydrocarbon chains depends upon the chemical type and length of the chain, the solvent or environment in which it immersed and the temperature [29].

In 1978, Goldenberg and Morawetz reported their research on the intramolecular excimer study of rate of conformational transitions. They studied the temperature of fluorescence behavior in low-viscosity media by using a series of compounds of type $ArCH_2XCH_2Ar$ (11) where Ar was phenyl, 1-naphtyl, or 4-biphenyl and X could be -CH_2-, -O-, or -NH_2^+-.

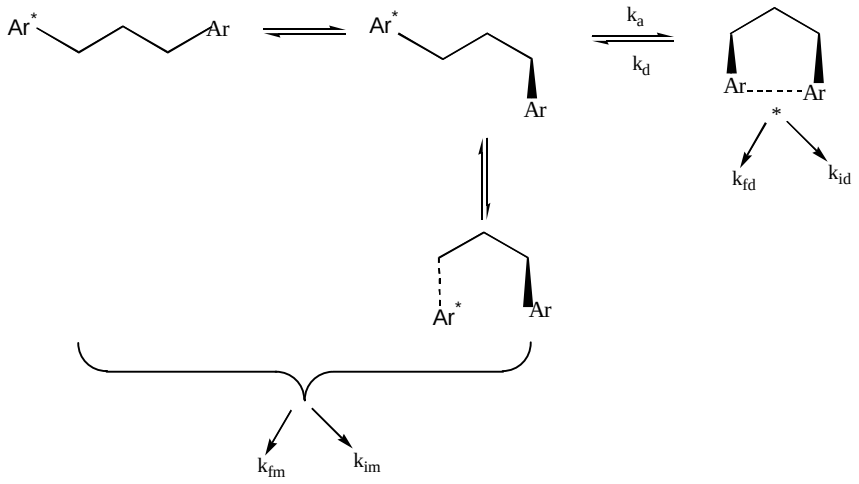

Figure 5. Monomer and dimer formations through bonds rotation

The intensity changes which characterizes the formation and deactivation of the intramolecular excimer state can be described by the above kinetic scheme. Here k_{fm} and k_{fd} are rate constants for fluorescence from monomer and excimer, k_{im} and k_{id} are the corresponding rate constants form internal quenching, while k_a and k_d characterize the

rates of intramolecular excimer formation and excimer dissociation. In the above scheme the rate constants for the radiative and nonradiative deactivation of the monomer do not depend on its conformational state. The solution of the rate equations assuming photostationary conditions leads to

$$I_d/I_m = Z\,(k_a/k_{fm})\,[1+(k_{id}+k_d)/k_{fd}]^{-1}a \qquad 11$$

Here Z relates the ratio of the peak heights to the ratio of the quantum yields of excimer and monomer emission, a is the fraction of the monomer in a conformation from which a single hindered rotation can lead to excimer formation.

The rate constants for the radiative emissions, k_{fm} and k_{fd} are independent of temperature while k_d is negligible and k_{id}/k_{fd} constant in the low temperature range of investigation. Sine the temperature dependence of a is much smaller than that of k_a , they obtained:

$$d \log (I_d/I_m)/d(1/T) = E_a/2.3R \qquad 12$$

where E_a is the activation energy for excimer formation and R is the gas constant.

In 1990, Eaton and Smart reported their study on the conformational study on the perfluorooctane chain [30]. They used temperature-dependent steady-state study (temperature changed from -10°C to 50°C) and equation 12. Steady-state values of the ratio I_d/I_m can be used to estimate the kinetic barrier to cyclization. Their data indicated

conclusively that the rate constant and the kinetic barrier for end-to-end cyclization were substantial different for the partially fluorinated molecule (**12**) and its corresponding hydrocarbon analog (**13**). The activation barrier difference is about 2.5 kcal/mol.

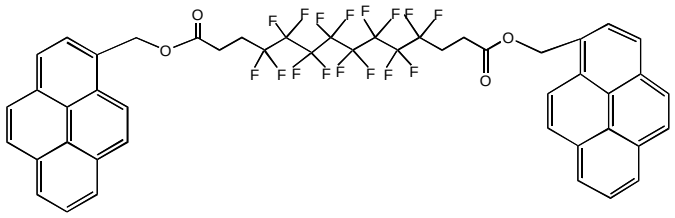

(12)

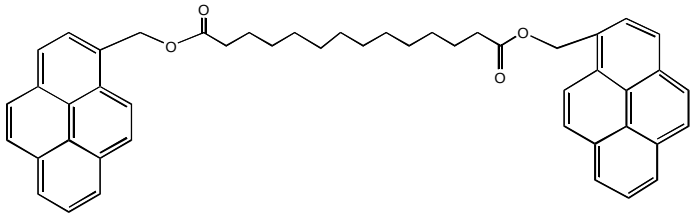

(13)

The objective of our research is to synthesize and study the conformational properties of a series of compounds that have different perfluoroalkane chains with two pyrene moieties on both ends and compare the differences with corresponding hydrocarbons. For this purpose, I synthesized and purified two series of compounds with general formula: Pyr-$(CF_2)_n$-Pyr (**14**) with n = 3,4,6 and Pyr-$(CH_2)_n$-Pyr (**8**) with n = 3. steady-state and temperature-dependent study had been performed on these molecules

and I am trying to determine the rotation barriers in perfluoroalkanes. The hydrocarbon molecules work as control compounds.

At high concentrations, the intermolecular excimer formation is the major event that takes place in the solution. But at very low concentrations, it is reasonable to assume that intramolecular excimer formation is the major one. The excimer formation of the di-pyrenylperfluoroalkane systems can be represented as in Figure 6.

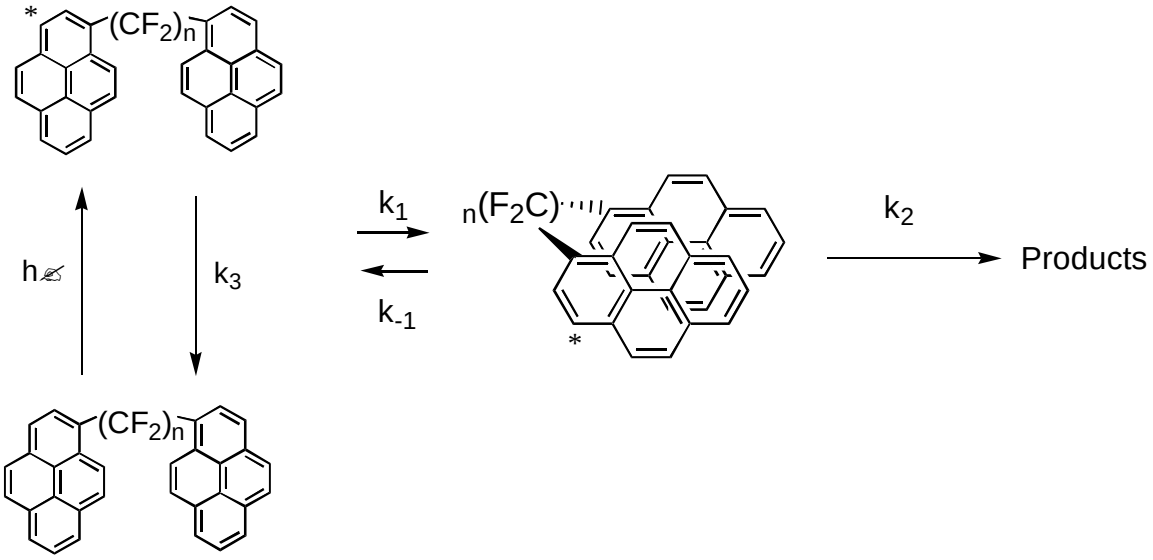

Figure 6. Schematic of the cyclization kinetic process.

The excimer formation kinetics of the perfluorodipyrenyl systems (14) can be represented as in figure 6 above. If the excited state species decays as the sum of two exponentials with decay constants $?_1$ and $?_2$ when k_{-1} and k_2 are comparable in magnitude, and if k_3 is the sum of first order rate constants for decay of the excited species that does not lead to cyclization,

$?_{1,2} = ½ \{(X+Y)?[(Y-X)^2 - 4k_1k_{-1}]^{1/2}\}$ 20

where $X= (k_1 +k_3)$ and $Y= (k_{-1}+k_2)$

The reaction is diffusion controlled when $4k_1k_{-1}$ is much smaller than $(Y-X)^2$. This occurs when k_{-1} is small.

The excimer kinetics of a pyrene-perfluoroalkane-pyrene unit (**14**) will depend to a very large extent on the perfluoroalkane chain's flexibility, the $F_2C–CF_2$ bonds will have to rotate to achieve the plane-parallel configuration to form the excimer. And the required rotational angle per $–CF_2–$ decreases as the chain length increases. Therefore, by studying an increasing number of $–CF_2–$ units linked between two 1-pyrenyl units, the excimer lifetime can be correlated to the number of $–CF_2–$ units.

1.4 Synthetic Scheme of Mono- and Di-pyrenyl perfluoroalkanes

Fluorocarbon compounds are almost entirely synthetic. However, selective functionalization of specific hydrogens remains challenging. Although there are a number of strategies for perfluoroalkylating an aromatic ring, the real challenge still lies in the controlled perfluoroalkylation of the aromatic rings.

One of the earliest known methods to prepare fluoroalkyl-substituted aromatic compounds is fluorination of fluoroalkyl aryl ketones with sulfur tetrafluorides [31]. The earliest known direct introduction of a fluoroalkyl group in aromatic compounds was thermolysis or peroxide-promoted thermolysis of perfluoroaklyl iodides [32]. Photolysis

of perfluoroalkyl iodide [33], hexafluoroacetone or perfluoroalkyl sulfonyl halides and also nickel carbonyl-promoted thermolysis of perfluoroacyl chlorides were later developments. The main disadvantage of these processes lies in the usage of vigorous conditions. Coe and Milner [34] reported a direct route to perfluoroalkyl benzenes under mild conditions using hexafluoropropylcopper species as reagents. From a synthetic viewpoint, this also has some drawbacks: (i) the usage of excess copper to generated organometallic reagent; (ii) a large stoichiometric excess of substrate to drive the reaction; and (iii) very low yields (5-30%) [35].

We primarily intended to synthesize the following series of the compounds: Pyr-$(CF_2)_n$-Pyr (**14**), Pyr-$(CH_2)_n$-Pyr (**15**), Pyr-$(CF_2)_n$-F (**16**). We decided to follow the direct method of preparation of the fluorocarbons (**14**) by a coupling reaction of 1-bromopyrene and the corresponding di-iodoperfluoroalkanes in the presence of copper (Scheme 1). The reactions proceeded to moderate yields in DMSO at 120^oC over 72hrs.

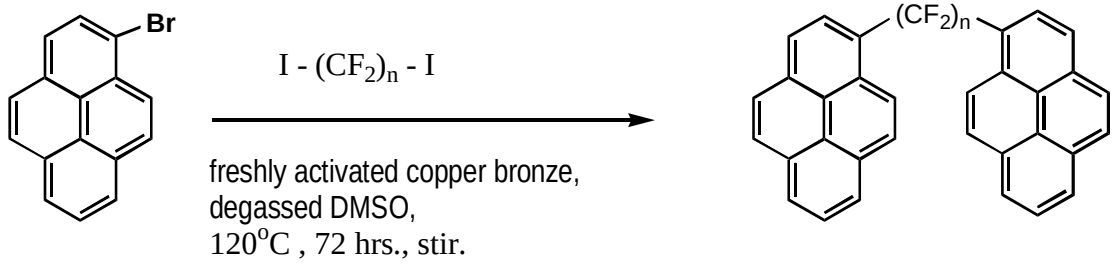

Scheme 1.

1,3-Di-iodohexafluoropropane, the starting material for the synthesis of **14** (n=3) was not available commercially and we had to adopt an alternate strategy for its synthesis. A novel 1,w-perfluoroalkylation of aromatic system (phenyl, tolyl) via bis-decarboxylation of perfluorodicarboxylic acids with XeF_2 was reported by Brel [36]. Direct decarboxylative alkylation of hexafluoroglutaric acid in the presence of pyrene was successful and afforded in 65% yield.

A similar strategy of coupling mono-iodoperfluoroalkanes with iodo- or bromopyrene was employed for the syntheses of the fluorocarbons (**15**), (Scheme 2).

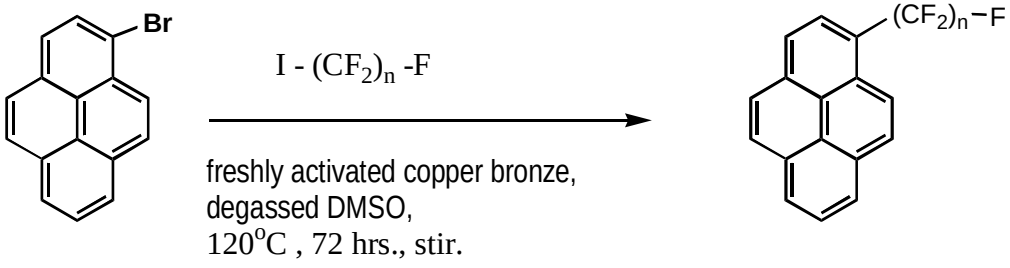

Scheme 2

The copper bronze obtained from Aldrich was activated using the standard procedure [36]. It turned out that using freshly activated copper was crucial for the yields and purification in these reactions.

Friedel-Crafts reaction with acetic anhydride reacted almost quantitatively to yield 1-acetylpyrene (**17**) which was then used for two separate reactions (Scheme 3).

The Aldol condensation product (**18**) with pyrene-1-carboxaldehyde on reduction gave the dimer with the three carbon chain (**19**).

The $NaBH_3CN/ZnI_2$ system was used for reducing [37] the Friedel-Crafts acylated ketones.

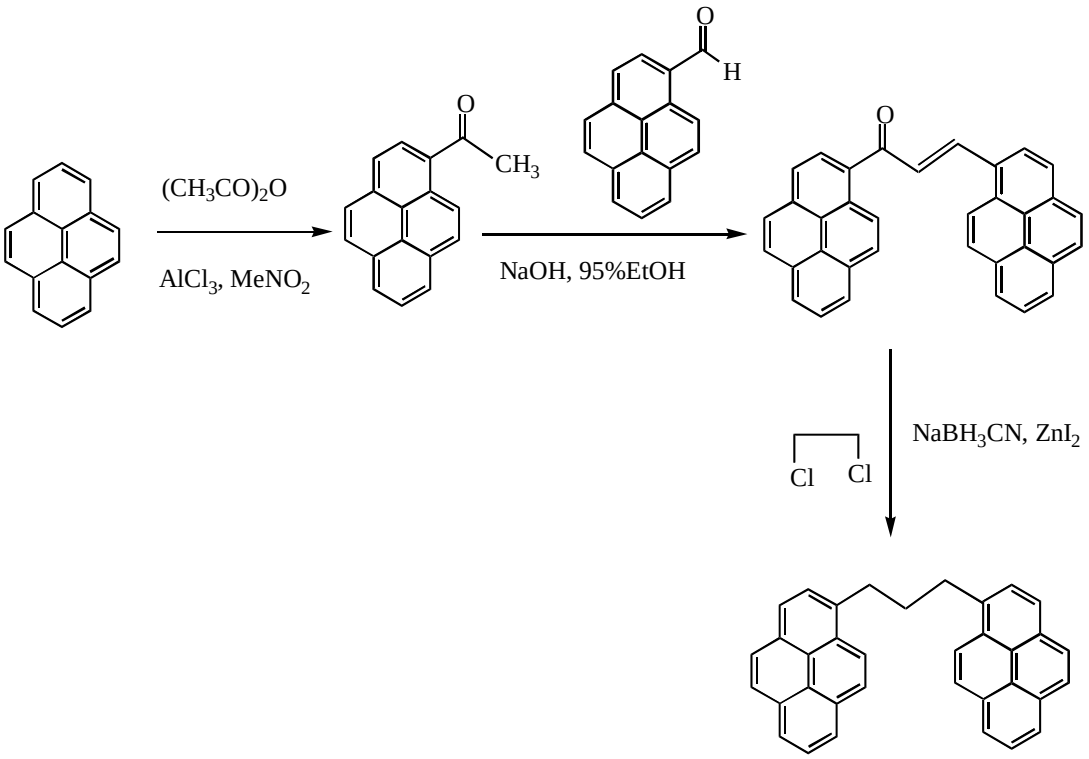

Scheme 3

Another scheme was employed using Grignard reagent to synthesize the P6HP compound.

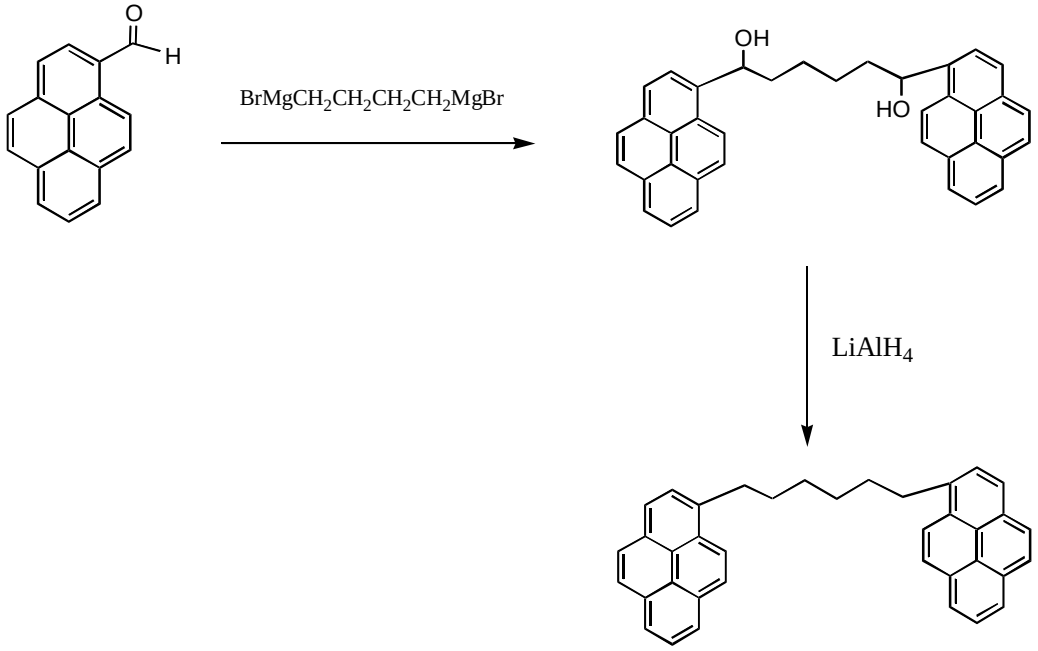

Scheme 4.

2. EXPERIMENTAL

The ^{1}H- and ^{13}C NMR spectra were recorded at 200 MHz and 50.4 MHz, respectively, on a Varian Gemini Fourier transform spectrometer (chemical shifts are relative to tetramethylsilane) and the ^{19}F spectra were recorded on a Varian 300 MHz Fourier transform spectrometer, scan frequency 282 MHz, (chemical shifts are relative to fluorotrichloromethane) at the Department of Chemistry NMR facility, University of North Texas. The HREI mass spectra were obtained from the Nebraska Center for Mass

Spectrometry, University of Nebraska, Lincoln, NE. The solvents pyridine and DMSO were dried by standard procedures from KOH and DMSO at reduced pressure over CaH_2. All yields were unoptimized. 1-Iodopyrene was synthesized by a Friedel-Craft reaction of pyrene with cyanogens iodide in the presence of $AlCl_3$.

Copper bronze obtained from Aldrich Chemicals Company was activated freshly by the standard procedure ----- 1.00g copper bronze was treated with a 10% solution of iodine in dry acetone utill the iodine color of the solution faded off; the copper was then filtered and washed three times with a 1:1 solution of concentrated HCl and dry acetone, followed twice by acetone and dried overnight in a vacuum dessicator over calcium chloride. The mono- and di-iodoperfluoroalkane starting materials were obtained from Lancaster Synthesis Inc.

2-(1-pyrenyl)ethane-2-one (17):

Degass nitromethane (50mL) for 2 hours and then add pyrene (0.5g, 2.47mmol) in and let it totally dissolve. And acetic anhydride (16, 0.23mL, 2.47mmol) is added. $AlCl_3$ (0.66g, 4.9mmol) is added while the reaction mixture was cooled in an ice bath. A dark solution formed. The reaction mixture is stirred at 70°C (bath temperature) for overnight, quench with ice and 1mL concentrated HCl. It is extracted in chloroform and the pure 2-(1-pyrenyl)ethane-2-one (**17**) is obtained after a silica gel column chromatograph using 5% of ethyl acetate in hexanes as eluent.

^{1}H NMR ($CDCl_3$, d ppm): 7.8-8.2 (m, 7H), 8.99-9.03 (br d, J = 9.9Hz, 2H), 2.8 (s, 3H).

1-[1-(prop-2-ene-1-one)pyrenyl]pyrene (18):

(1-pyrenyl)ethane-2-one (**17**, 0.217 g, 0.9 mmol), and pyrene-1-carboxaldehyde (**19**, 0.200 g, 0.9 mmol) are refluxed in 95% ethanol/water overnight to give 1-[1-(prop-2-ene-1-one)pyrenyl]pyrene (18). Purify the compound with column chromatograph using 5% of ethyl acetate in hexanes as eluent, pure compound is obtained.

^{1}H NMR ($CDCl_3$, d ppm): 8-8.35 (m, 5H), 8.79-8.80 (br d, J=8.4 Hz, 2H), 9.94-9.96(br d, J=10 Hz, 2H), 7.88-7.89(br d J=20 Hz, 2H).

^{13}C NMR ($CDCl_3$, d ppm): 123.8, 125.0, 126.1, 126.5, 127.0, 128.0, 129.0, 130.2, 131.5, 132.2, 137.0, 194, 142.5, 150.0.

1-[1,3-di-(1-pyrenyl)propyl]pyrene (20, P3HP):

1-[1-(prop-2-ene-1-one)pyrenyl]pyrene (**19**, 0.150 g, 0.3 mmol), sodium cyanoborohydride (**21**, 0.417 g, 6.6 mmol) and zinc iodide (**22**, 0.427 g, 2.2 mmol) are dissolved in 1,2-dichloroethane (50 mL) and stir at room temperature for 48 hours to give P3HP. P3HP is purified by column chromatography in silica gel using 5% of ethyl acetate in hexanes as eluent.

^{1}H NMR ($CDCl_3$, d ppm): 8-8.25 (m, 7H), 7.9-7.95 (br d, J=10 Hz, 2H), 3.45-3.55 (t, J=10 Hz, 4H), 2.39-2.56 (m,2H).

^{13}C NMR ($CDCl_3$, d ppm): 33.7, 33.9, 123.8, 125.0, 126.1, 126.5, 127.0, 128.0, 129.0, 130.2, 131.5, 132.2, 137.0.

1-[1,1,2,2,3,3,4,4,5,5,6,6,-dodecafluoro-6-(1-pyrenyl) hexyl]pyrene (23, P6FP):

Synthesis and purification of P6FP was carried out using 1-bromopyrene (**24**, 500 mg, 1.5 mmol), 1,6-diiodoperfluorohexane (**25**, 415.4 mg, 0.75 mmol) and copper bronze (**26**, 315 mg, 5 mmol) in DMSO (4 mL). The yield is 37.9 % (200 mg) with respect to 1,6-diiodoperfluorohexane. The pure compound is obtained by purifying with column chromatograph in silica gel using 5% of ethyl acetate in hexanes as eluent.

^{1}H NMR (CDCl3, d ppm): 7.95-8.30 (m, 14 H), 8.45-8.50 (br d, J = 10.4 Hz, 4H).

^{19}F NMR (CFCl3, d ppm): -103.02, -120.12, -121.28.

Mass (M/z): (HREI): Found M+. = 702.1207 Calcd. for $C_{38}H_{18}F_{12}$ (702.1217).

1-[1,1,2,2,3,3,4,4-octafluoro-4-(1-pyrenyl)butyl]pyrene (27, P4FP):

Synthesis and purification of P4FP was carried out as 23 using 1-bromopyrene (**24**, 500 mg, 1.5 mmol), 1,4-diiodoctafluorobutane (**28**, 340.4 mg, 0.75 mmol) and copper bronze (**26**, 315 mg, 5 mmol) in DMSO (4 mL). The yield is 33.4 % (150 mg) with respect to 1,4-diiodoctafluorobutane. The compound is purified by column chromatorgraph in silica gel using 5% of ethyl acetate in hexanes as eluent.

^{1}H NMR (CDCl3, d ppm): 7.9-8.3 (m, 14H), 8.3-8.4 (d, J = 8.4 Hz, 4H).

^{19}F NMR (CFCl3, d ppm): -100.717, -113.577.

Mass (M/z): (HREI): Found M^{+} = 602.3, Calcd. For $C_{36}H_{18}F_{8}$ (602.1781).

1-[1,1,2,2,3,3-hexafluoro-4-(1-pyrenyl)butyl]pyrene (29, P3FP):

To a solution of hexafluoroglutaric acid (**30**, 500mg, 2.11 mmol) and pyrene (**6**, 1.8 g, 9mmol) in dry dichloromethane (20ml) is added XeF_2 (**31**, 360mg, 2.11mmol). The mixture is stirred at 10-20C for 3.5hr and treated with aqueous bicarbonated solution.

The pure compound is obtained by flash chromatorgraphy using 5% of ethyl acetate in hexanes (754mg, 65%).

^{1}H NMR (CDCl3, d ppm): 8.0-8.30 (m,14H), 8.32-8.42 (br d, J=10.2Hz,4H).

^{19}F NMR (CDCl3, d ppm): -123.305, -124.289.

Mass (M/z): (HREI): Found M^{+} = 552.1310 Calcd. For $C_{35}H_{18}F_{6}$ (552.1313).

1-[1,1,2,2,3,3,4,4,5,5,6,6,6-tridecafluorohexy]pyrene (32, P6FF):

A mixture of 1-iodopyene (**33**, 500mg, 1.5 mmol), copper bronze (**26**, 63mg, 1mmol), and 1-iodoperfluorohexane (**34**, 0.12ml, 2.47mmol) in pyridine (1ml) is heated for 72hrs at 80°C under a positive pressure of nitrogen. It is then filtered through a short pad of celite and the resulting dark solution is chromatographed with chloroform. The fastest moving fraction is collected and is rechromatographed using a precoated TLC plate (silica gel 20cm x 20cm, 500 microns). Elution with 10% ethyl acetate in hexanes yield yellow crystals of P6FF (240mg, 31%). Crystals of **33** were recovered after the reaction.

^{1}H NMR (CDCl3, d ppm): 7.85-8.20 (m, 7H), 8.40-8.50 (br d, J=8.14Hz, 2H).

^{13}C NMR (CDCl3, d ppm): 96.22, 124.88, 125.34, 125.69, 125.79, 125.83, 126.33, 126.96, 127.32, 127.86, 129.25, 130.87, 131.07, 131.26, 136.69.

^{19}F NMR (CDCl3, d ppm): -81.34, -103.38, -120.52, -121.99, -123.28, -126.71.

Mass (M/z): (HREI): Found M^{+} = 520.0496 Calcd. For $C_{22}H_{9}F_{13}$ (520.0496).

1-[1,1,2,2,3,3,4,4,4-nonafluorobutyl]pyrene (35, P4FF):

Synthesis of **35** is carried out as described for 3**2** using 1-iodopyene (**33**, 200mg, 0.6 mmol), 1-iodononafluorobutane (**36**, 210mg, 0.6 mmol), and copper bronze (**26**, 63mg, 1mmol) in DMSO (1ml) and allowed to react for 72hrs. Yield of **35** was 37% (95mg). **33** was recovered after the reaction.

^{1}H NMR (CDCl3, d ppm): 7.9-8.1 (m, 7H), 8.3-8.55 (br d, J=10.4Hz, 2H).

^{19}F NMR (CDCl3, d ppm): -93.7, -111.5, -118.5, -131.8.

Mass (M/z): (HREI): Found M^{+} = 420.0567 Calcd. For $C_{20}H_9F_9$ (420.0560).

8-(1,4- dimethoxy-2-naphthyl) -1,4-dioxaspiro[2,5]decan-8-ol (37):

1,4-dimethoxy-2-bromonahthalene (**38**, 1.0g, 3.74mmol) is dissolved in dry THF. Magnesium powder (0.25g, 10.4mmol) and a small piece of iodine are added and the resulting mixture is stirred for 0.5 hr. The mixture of 1,4-cyclohexanedione monoethyleneketyl (**39**, 0.6g, 3.78mmol) in dry THF is added dropwise over 20 mins. The reaction mixture is stirred further for 2 hrs and poured into ice-cold water. The product is extracted with CH_2Cl_2 and dried over magnesium sulfate. Evaporate the solvent and use 20% of ethylacetate in hexanes as elution to separate out the product (1.0g, yield is 78%).

^{1}HNMR (CDCl3, d ppm): 1.5-2.4 (m, 8H), 3.99 (s, 3H), 4.01 (s, 4H), 4.02 (s, 3H) 5.01(s, 1H), 6.75 (s, 1H), 7.45-7.60 (m, 2H), 7.96-8.02 (m, 1H), 8.18-8.25 (m, 1H).

8-(1,4- dimethoxy-2-naphthyl)-1,4-dioxaspiro[2,5]decan-7-ene (40):

The mixture of 1.0g (2.9mmol) 8-(1,4- dimethoxy-2-naphthyl) -1,4-dioxaspiro[2,5]decan-8-ol (**37**), an excess amount of acetic anhydride and 1 gram of

sodium bicarbonate is heated up to 200°C and refluxed for 2 hrs. Then the solid is filtered out and ethyl acetate is used to wash the solid. The solvent is washed by salt saturated sodium bicarbonate solution and extracted with ethyl ether and dried with the sodium bicarbonate solid. The solvent is removed under reduced pressure. The pure product (0.807g, yield is 85.2%) was obtained by column chromatography (use 20% of ethyl acetate in hexanes as eluent).

^{1}HNMR (CDCl3, d ppm): 1.96 (m, 2H), 2.52 (m, 2H), 2.77 (m, 2H), 3.82 (s, 4H), 3.98 (s, 3H), 4.05 (s, 3H), 5.63 (s, 1H), 5.64 (m, 1H), 7.4-7.6 (m, 2H), 8.05-8.25 (m, 2H).

GC-MS: 326 (M^+).

8-(1,4- dimethoxy-2-naphthyl)-1,4-dioxaspiro[2,5]decane (38):

Dissolve 1.40g (4.3mmol) 8-(1,4- dimethoxy-2-naphthyl)-1,4-dioxaspiro[2,5]decan-7-ene (37) in THF and add platium on activated carbon and add hydrogen from a balloon, stir at room temperature overnight. Filter off the solid and pure product (1.143g, yield is 81.2%) is obtained by column chromatography (20% of ethyl acetate in hexanes as eluent).

M.P.: 129-129.5°C

^{1}HNMR (CDCl3, d ppm): 1.5-2.0 (m, 8H), 3.2-33 (m, 1H), 3.86 (s, 4H), 3.98 (s, 3H), 4.0 (s, 3H), 6.66 (s, 1H), 7.35-7.55 (m, 2H), 8.0 (m, 1H), 8.2 (m, 1H).

4-(1,4- dimethoxy-2-naphthyl)-cyclohexanone (39):

0.943g (2.88mmol) of 8-(1,4- dimethoxy-2-naphthyl)-1,4-dioxaspiro[2,5]decane (**38**) is dissolved in THF and a mixture of 80% aqueous acetic acid is added. Maintain

the refluxing temperature for 1 hr. The reaction is quenched by pouring the reaction mixture into 100 ml of ice-cold saturated aqueous sodium bicarbonate solution. Extract with ether in the usual manner. Pure product (0.817g, yield is 96%) is obtained by column chromatograph (20% of ethyl acetate in hexanes as elution).

M.P.: 139.5-141°C

^{1}HNMR (CDCl3, d ppm): 2.0-2.3 (m, 4H), 2.5-2.8 (m, 4H), 3.6-3.8 (m, 1H), 3.94 (s, 3H), 3.98(s, 3H), 6.6(s, 1H), 7.4-7.6(m, 2H), 8.0(m, 1H), 8.25(m, 1H).

4-(1,4- dimethoxy-2-naphthyl)-cyclohexanol (40):

Dissolve 0.5g (1.76mmol) of the 4-(1,4- dimethoxy-2-naphthyl)-cyclohexanone (**39**) in 10ml THF. Add 150mg (3.97mmol) sodium borohydride in 10 ml 85% ethanol in water. Pour the sodium borohydride solution in the starting material in THF. Stir at room temperature overnight. At the beginning, the solution is clear, after the reaction, lots of solid come out. Filter the solid out and remove the solvent. The pure product (0.478g, yield is 95.1%) is obtained by column chromatography (10% of ethyl acetate in hexanes as elution).

^{1}HNMR (CDCl3, d ppm): 1.44-2.2 (m, 8 H), 3.1-3.3 (m,1H), 3.65-3.8 (m, 1H), 3.86 (s, 3H), 3.96 (s, 3H), 6.59 (s, 1H), 7.35-7.55 (m, 2H), 8.20 (m, 1H).

4-(1,4- dimethoxy-2-naphthyl)-bromocyclohexane (41):

Dissolve 0.286g (1.0mmol) of 4-(1,4- dimethoxy-2-naphthyl)-cyclohexanol (**40**), 0.42g (1.6mmol) of triphenylphosphine, and 0.531g (1.6mmol) of carbon tetrabromide in

20ml of acetonitrile. The reaction mixture is heated up to 130°C and stir overnight. Remove the solvent and pure product (0.16g, yield is 46%) is obtained by column chromatography (10% of ethyl acetate in hexanes as elution).

^{1}HNMR (CDCl3, d ppm): 1.6-2.4 (m, 8H), 3.2-3.4 (m, 1H), 3.9 (s, 3H), 4.06 (s, 3H), 4.84 (m, 1H), 6.80 (s, 1H), 7.4-7.62 (m, 2H), 8.0-8.4 (m, 2H)

^{13}CNMR (CDCl3, d ppm): 28.46, 35.58, 37.00, 54.95, 56.21, 63.09, 103.11, 122.52, 122.81, 125.38, 127.02, 126.00, 129.20, 134.80, 146.40, 152.80.

3. RESULTS AND DISCUSSION

3.1 Synthesis and Characterization of the Hydrocarbon Compounds

The Friedel-Crafts acylation of pyrene followed by reduction was a general procedure that gave P3HP successfully. Pyrene reacted with acetic anhydride using nitromethane as solvent. The reaction was quantitative, but the only problem was that pyrene did not dissolve much in nitromethane. So, the same reaction was tried using nitrobenzene as solvent. But due to the purification problem, nitromethane was used as reaction solvent at last. Another reason I use nitromethane is that the product dissolved in it very well and it favored the equilibrium towards product eventually. Pyrene and acetic anhydride were mixed together in an ice bath first and $AlCl_3$ as catalyst which must be over amount, about 1.1 equivalent. Unlike Friedel-Crafts alkylation, acylation consumed $AlCl_3$. The ^{1}HNMR of Pyr-$COCH_3$ showed that hydrogen adjacent to the

substituted position that showed the doublet shifted downfield with respect to other hydrogens on the pyrene. The carbonyl group exerted an induction effect that is responsible for this deshielding. I tried this reaction several times and found out that the amount of $AlCl_3$ was very important because the Friedel-Crafts reaction was sensitive to the amount of catalyst used. If the amount of the $AlCl_3$ is less than 1 equivalent, it is hard to get the optimized amount of product. The amount of $AlCl_3$ should be at least 1.1 equivalents. But an excess of catalyst resulted in a black precipitate which was hard to filter out and some product was lost during filtration the catalyst out. I had to use a layer of celite to get rid of the black solid. According the literature, $AlCl_3$ should be added before the anhydride was dripped in. But what I found is that, the sequence of adding reactants in this reaction is not very important. The yield of this reaction is 67%. Some unreacted pyrene was left over.

The next step was an aldol condensation reaction. It is a straightforward reaction. The product was made by a straight reaction of Pyr-$COCH_3$ and pyrene-1-carboxaldehyde in 1:1 ratio and in the presence of sodium hydroxide solid in 95% ethanol water solution under refluxing. Prolonged reaction time result better yield. The olefinic protons were observed at 5.4 ppm.

The last step towards the synthesis of compound P3HP was a reduction reaction. We used the reduction reagent $NaBH_3CN$ in the reaction. This reduction is a very high yielding reaction and the reaction condition was much milder than the reference mentioned. Large access of sodium cyanoborohydride and zinc iodide (in ratio of 2:1) was added to reaction mixture and stirred at room temperature for 48 hrs in 90%. Prolonged reaction time increased percent yield.

The pyrene acylation reaction was not easy to control in the synthesis of compound P6HP. In the reference [**27**], they used the aldol condensation reaction. We tried, but only got one side of the compound $CH_3COCH_2CH_3$ reacted with Pyr-CHO. The other side of the ketone did not. We modified the reactants to $CH_3COCOCH_3$ and let it react with Pyr-CHO. And hoped that both sides of the 2,3-butanedione would react. The compounds were added in 2:1 fashion and use NaOH as base. But, it turned out that the only product we got did not have a carbonyl stretch in the FT-IR spectra.

Another method [**37**] was to use Grignard reagent of 1,4-dibromobutane to react with pyrene-1-carboxyaldehyde. We should be able to get a dialcohol and then use $LiAlH_4$ as the reducing reagent to reduce the -OH group to -H. In a literature search, we found that the 1,4-dibromobutane could form the cyclobutane when making the Grignard reagent on both sides. So, we used a little larger amount of dibromobutane to make the Grignard reagent. If part of the molecules form the cyclobutane, it would not affect the final purification. We tried this method, but found out that the final product we need was the minor one and we could not accumulate enough amount to do the spectroscopy study.

3.2 Syntheses and Characterization of the Fluorocarbon Compounds

1-bromopyrene and the 1,6-diiodoperfluorohaxane were reacted in a 2:1 molar ratio with five times excess copper in DMSO at 120°C over 72 h. to give P6FP (**23**). The reaction proceeded to a moderate yield of 37.9% with respect to 1,6-diiodoperfluorohaxane, unoptimised. The product P6FP (**23**) was fully characterised using ^{19}F- and ^{1}H NMR and Mass spectrometry. The three fluorine peaks at -103.02, -

120.12, -121.28 ppm correspond to d -, ß- and ?-CF_2 respectively. The molecule is symmetrical about the ? -CF_2. The ^{1}H-NMR spectrum shows that the aromatic protons are shifted downfield from pyrene and a large (0.4ppm) downfield shift in the position of H2/H3 doublet, with respect to the other aromatic protons due to the inductive effect of the perfluoroalkyl group as well as its steric crowding which adds to the deshielding of the aromatic protons. The HREI mass ion peak of 702.1207 was observed corresponding to the molecular ion.

P4FP (**27**) was similarly prepared by reacting 1-bromopyrene with 1,4-diiodooctafluoro butane in 2:1 molar ratio with 5 mole equivalents of copper, in DMSO. Carrying out the reaction at 120°C over 72 hrs gives a 33.4% yield of 20 with respect to 1,4- diiodooctafluoro butane, unoptimised. The molecule is symmetrical about the ß -CF_2 group, which is evident from the observation of two fluorine peaks at -100.717 and -113.577 ppm, corresponding to the d- and ß- CF_2, respectively. In the ^{1}HNMR spectrum, the aromatic protons are shifted downfield from pyrene. A downfield shift (0.4ppm) in the position of H2/H3 doublet, with respect to the other aromatic protons, at 8.3-8.4ppm is due to the inductive and steric effects of the perfluoroalkyl group. The LREI mass ion peak of 602.3 was observed corresponding to the molecular ion. .

P4FF (**35**) was similarly obtained in a 48.8% yield on reacting 1-bromopyrene with 1-iodononafluorobutane in a 1:1 molar ratio, in DMSO at 120 °C over 72 hrs.. The ?- CF_2 peak appeared at -93.7 ppm in the ^{19}F NMR and the -CF_3 peak appeared at -131.8 ppm while the ?- and ?- CF_2 appeared at -111.5 and -118.5 ppm, respectively. The H2/H3 coupling was of 10.4Hz and was shifted downfield with respect to the aromatic protons by 0.4 ppm. The HREI mass ion peak of 420.0567 was observed corresponding

to the molecular ion. Other identified fragments included the peak with mass 251, which corresponds to the formation of Pyr-CF_2 by benzylic fragmentation.

The melting points of all the fluorinated pyrenes were greater than 200 $^{\circ}$C and the materials were stable and not sensitive to moisture or light.

To avoid forming the complex mixture of products on carrying out the reactions at the elevated temperatures, other solvents were tried. Pyridine is known to give acceptable yields in these reactions at lower temperatures. The coupling was facile with pyridine, at lower temperatures of 85-95°C, and the yield was comparable to that in DMSO. Using a 1:1 mixture of pyridine and HMPA did not alter the yields to a very large extent.

3.3 Fluorescence spectroscopies of hydrocarbon and fluorocarbon compounds

All the solvents used were spectroscopy grade without further purification and seals were opened inside the glove box. All the compounds were purified again before using. The amount needed was weighed and put in the volumetric flasks and were desiccated in the drying chamber overnight before being transferred into the glove box. And all the solutions were prepared in the glove box filled with argon gas.

After the solutions were prepared, they were transferred again into the cells (Starna Cells, 23-Q-10 quartz fluorometer cell, rectangular) inside the glove box, sealed with parafilm. The maximum absorptions of the compounds were obtained with a HEWLETT PACKARD 8453 spectrophotometer. First the background of the solvent was collected by putting methylcyclohexane solvent in a clean cell. Then the solutions

were checked and maximum absorptions were read from the given spectra which subtracted the background automatically.

The steady-state fluorescence spectra of compounds were obtained with a FS900CDT T-Geometry Fluorometer and the source of light was a xeon short arc lamp made by Edinburgh Analytical Instruments (EAI). All the slits were set to 0 mm at first. The cooling system was set to -30 ± 0.5ºC which made the light sensor stabilized. Under these conditions, the background should be under 100 counts. Put the samples in the sample holders. Set the excitation slits to 0.25 mm and the excitation wavelength to the maximum absorptions of the samples. Adjust the emission slits and let the count number be 3000 ± 150. Usually, the slits openning were also in the range of 0.25-0.35 mm, depending on the concentrations of the solutions. Then, began collecting the fluorescence spectra of the samples from 350 to 600 nm with a step of 1nm.

To all the pyrene compounds with perfluorocarbon chains, there were three groups of maximum excitation (250-298nm, 300-325nm, 326-349nm). and the group around 343nm was always the one that be chosen to run the fluorescence spectra by references[17, 27]. So, we picked up 343 as the maximum excitation. And first of all, we checked the absorbance of every compound in low concentrations and we also could make sure that the pyrene compounds obeying Beer's law in all of it range we chose. Following are the data we got.

Compound	Wavelength (nm)	Absorbance	Concentration (M)	Molar absorptions ($cm^{-1}M^{-1}$)	Average (e) ($cm^{-1}M^{-1}$)	?
P3HP	344	0.77	$1.8*10^{-5}$	$4.3*10^{4}$		
P3HP	344	0.4	$9.0*10^{-6}$	$4.4*10^{4}$	$5.1*10^{4}$	0.23
P3HP	344	0.058	$9.0*10^{-7}$	$6.4*10^{4}$		
P3FP	343	2.69	$2.4*10^{-5}$	$1.1*10^{4}$		
P3FP	343	0.22	$2.4*10^{-6}$	$9*10^{3}$	$9.3*10^{3}$	0.161
P3FP	343	0.019	$2.4*10^{-7}$	$8*10^{3}$		
P4FF	343	2.29	$2.57*10^{-5}$	$8.9*10^{4}$		
P4FF	343	0.24	$2.57*10^{-6}$	$9.3*10^{4}$	$1.0*10^{5}$	0.131
P4FF	343	0.03	$2.57*10^{-7}$	$1.2*10^{5}$		
P4FP	343	0.72	$4.6*10^{-5}$	$1.6*10^{4}$		
P4FP	343	0.13	$9.2*10^{-6}$	$1.4*10^{4}$	$1.6*10^{4}$	0.098
P4FP	343	0.08	$4.6*10^{-6}$	$1.7*10^{4}$		
P6FF	343	1.88	$5*10^{-5}$	$3.8*10^{4}$		
P6FF	343	0.20	$5*10^{-6}$	$4*10^{4}$	$4.4*10^{4}$	0.286
P6FF	343	0.027	$5*10^{-7}$	$5.4*10^{4}$		
P6FP	343	0.78	$2.8*10^{-5}$	$2.8*10^{4}$		
P6FP	343	0.19	$5.6*10^{-6}$	$3.4*10^{4}$	$3.1*10^{4}$	0.102
P6FP	343	0.085	$2.8*10^{-6}$	$3*10^{4}$		

Table 1. The molar absorbance coefficients of compounds we used.

Concentrations (M)	$4*10^{-5}$	$9.4*10^{-6}$	$2.3*10^{-6}$
Absorbance	1.35	0.29	0.07

Table 2. Absorbance of P6FP at wavelength 343 in various concentrations

Concentrations (M)	$6.0*10^{-4}$	$1.18*10^{-4}$	$2.4*10^{-5}$
Absorbance	>3	1.88	0.39

Table 3. Absorbance of P4FP at wavelength 343 in various concentrations

Concentrations (M)	$2.8*10^{-5}$	$2.1*10^{-5}$	$4.8*10^{-6}$
Absorbance	2.777	2.136	0.48

Table 4. Absorbance of P4FF at wavelength 344 in various concentrations

Concentrations (M)	$1.1*10^{-4}$	$2.6*10^{-5}$	$5.4*10^{-6}$
Absorbance	1.02	0.24	0.05

Table 5. Absorbance of P3FP at wavelength 343 in various concentrations

From the above tables, when the concentrations of compounds decreased in very dilute solution (in 10^{-4} and 10^{-5} scale), the absorbance of these compounds decreased

correspondingly in the same magnitude. This means these compounds obey Beer's law in the ranges chosen. The Beer's law data indicate that ground state dimmer formation is not important at the low concentration we chose for the emission measurement.

The fluorescence data of fluorocarbons with different concentrations are listed below.

Concentration (M)	Peak Height (@397nm)	Peak Height (@448nm)
$1.2*10^{-5}$	$2.706*10^{4}$	$2.267*10^{4}$
$2.4*10^{-6}$	$2.667*10^{4}$	$9.233*10^{3}$

Table 6. The fluorescence variations of P6FF with various concentrations

Concentration (M)	Peak Height (@397nm)	Peak Height (@448nm)
$3.3*10^{-5}$	$3.072*10^{4}$	$2.028*10^{4}$
$1.1*10^{-6}$	$2.733*10^{4}$	$1.458*10^{4}$

Table 7. The fluorescence variations of P6FP with various concentrations

Concentration (M)	Peak Height (@396nm)	Peak Height (@450nm)
$1.63*10^{-4}$	$4.50*10^{3}$	$7.34*10^{2}$
$4.23*10^{-5}$	$3.121*10^{3}$	$1.99*10^{2}$
$1.04*10^{-5}$	$2.739*10^{3}$	$1.49*10^{2}$

Table 8. The fluorescence variations of P4FF with various concentrations

Concentration (M)	Peak Height (@410nm)	Peak Height (@512nm)
$1.8*10^{-5}$	$2.77*10^{4}$	$2.44*10^{4}$
$3.6*10^{-6}$	$2.39*10^{4}$	$2.42*10^{4}$

Table 9. The fluorescence variations of P3HP with various concentrations

From the steady-state fluorescence data of mono-substituted fluorocarbon of P6FF, we can see that when the concentrations of fluorocarbons decreased, the ratio of dimer to monomer peaks changed dramatically. From the data of di-substituted fluorocarbons P6FP, when the concentrations of fluorocarbons decreased, the ratio of dimer to monomer peaks did not significantly change. This means that excimer formation for the fluorinated pyrene monomers is highly dependent on the concentration and is less efficient than that for pyrene. Excimer formation for the fluorinated pyrene dimers is efficient and only slightly concentration dependent.

As for the temperature dependent study, I first set the temperature of the water bath to 5ºC. The minimum temperature in the cell holder can be as low as 11ºC. After the temperature stabilized, the spectra were obtained. Then, the next temperature was set. Usually the interval is ten-Celsius degrees. The highest water bath temperature I could used was 60ºC. The highest usable temperature in the cell holder could go up to 51ºC.

The temperature-dependent fluorescence study data of di-substituted fluorocarbons are listed below.

Wavelength(nm) / temperature	376	443	Ratio of 443 to376
11.0	$1.948*10^4$	$0.6618*10^4$	0.340
25.6	$1.581*10^4$	$0.6067*10^4$	0.384
34.6	$1.467*10^4$	$0.5980*10^4$	0.408
51.0	$1.412*10^4$	$0.5826*10^4$	0.413

Table 10. The fluorescence variations of P6FP with various temperatures

Wavelength(nm) / Temperature(°C)	378	448	Ratio of 448 to378
11.2	$2.194*10^4$	$2.344*10^3$	0.107
22.2	$1.944*10^4$	$2.154*10^3$	0.111
33.6	$1.845*10^4$	$1.941*10^3$	0.105
51.0	$1.434*10^4$	$1.558*10^3$	0.109

Table 11. The fluorescence variations of P4FP with various temperatures

Wavelength(nm) / Temperature(°C)	380	448	Ratio of 448 to380
12.2	$1.627*10^3$	$6.995*10^3$	4.230
16.8	$1.618*10^3$	$6.984*10^3$	4.310
27.0	$1.528*10^3$	$6.833*10^3$	4.464
41.2	$1.461*10^3$	$6.659*10^3$	4.566
51.0	$1.554*10^3$	$6.647*10^3$	4.219

Table 12. The fluorescence variations of P3FP with various temperatures

Wavelength(nm) / Temperature(°C)	395	512	Ratio of 512 to395
14.3	$2.73*10^4$	$2.34*10^4$	0.862
18.6	$2.70*10^4$	$2.31*10^4$	0.854
25.4	$2.63*10^4$	$2.17*10^4$	0.826
33.2	$2.83*10^4$	$2.32*10^4$	0.820
48.4	$2.73*10^4$	$2.36*10^4$	0.862

Table 13. The fluorescence variations of P3HP with various temperatures

From these data, we can see that, with the change of temperature, the ratios of the dimer and monomer peaks of some of the compounds show certain tendencies. This meant that because of the stiffness of the perfluorocarbon chain, even though we raised the temperature, the excimer formation for the fluorocarbon dimers did not change much. Another factor that might affect the dimer formation is concentration. Since all the substances are in very low concentration (in 10^{-5} M scale), the formation of intermolecular dimers is very unlikely. When we changed the temperature, more molecules will have sufficient energy to leave their most stable conformation and the fluorescence peak height decrease a little bit. (All the peak heights decrease when I increase the temperatue, but I haven't thought out the reason yet. But the ratio of P6FP increases.) The ratios of the peak height depend on the fluorocarbon. P3FP has the highest ratio and P4FP has the lowest ratio. The reason P3FP has the highest dimer peak height is due to the chain length favoring the dimer formation. Even though we raise the

temperature and the concentration, the dimer peak height does not significantly change. P4FP has the lowest dimer peak height which means that the chain length discourages the dimer formation. And the chain length of P6FP is the longest among these compounds, so the stiffness of the chain might not be as great, which would allow it to dimerize more than P4FP.

REFERENCES

1. TEFLON PFA FLUOROCARBON RESIN-WEAR AND FRICTIONAL DATA, APD#2, BULLETIN, E.I. DUPONT DE NEMOURS& CO. INC. WILMINGTON, DE, 1973.

2. BOWERS, R.C.; BISMAN, W.A., *IND. CHEM. PROD. RES.* , 1974, **13**, 115

3. PACE, E.L., ASTON, J.G., J. AM. CHEN. SOC. 1948, **70**, 566

4. ADAMS, R. AND YUAN, H. C., *CHEM. REV.*, 1933, **12**, 261

5. BO? SEKEN, J. AND COHEN, R. *REC. TRAV. CHIM.*, 1928, **47**, 839

6. WOLF, K.L., *TRANS. FARADAY SOC.*, 1930, **26**, 315

7. MIZUSHIMA, S. AND HIGASI, K., *J. CHEM. SOC. JAPAN*, 1933, **54**, 226

8. KEMP, J.D., PITZER, K.S., *J. CHEM. PHYS.*, 1936, **5**, 473

9. WITT, R.K. AND KEMP, J.D., *J. AM. CHEM. SOC.*, 1973, **59**, 273

10. BERG. U., SANDSTROM, *J. ADV. PHYS. ORG. CHEM.*, 1989, **25**, 1-97

11. ELIEL, E.L.; ALLINGER, N.L.; ANGYAL, S.J.; MORRISON, G.A., *CONFORMATIONAL ANALYSIS*, JOHN WILEY & SONS, INC

12. PACE, E.L. AND ASTON, J.G., *J.AM.CHEM.SOC.*, 1948, **70**, 566

13. PITZER, R.M., *J. CHEM. PHYS.*, 1973, **5**, 469

14. SCHASFER, T., AND SEBASTIAN, R.,VERGIN, R.P., LAATIKAINEN, R., *CAN. J. CHEM.*, 1983, **29**, 61

15. BIRKS, J. B. *PHOTOPHYSICS OF AROMATIC MOLECULES*; WILEY INTERSCIENCE, LONDON, 1970.

16. LAKOWICZ, J. R., *PRINCIPLE OF FLUORESCENCE SPECTROSCOPY*, 2ND ED., KLUWER ACADEMIC/PLENUM PUBLISHERS, NY, 1999

17. FÖRSTER, TH., *ANG. CHEM. INT. ED. ENG.*, 1969, **8**, 333

18. STEVENS, B.; BAN, M. I., *TRANS. FARADY SOC.*, 1964, **60**, 1515.

19. FÖRSTER, T. AND KASPER, K., *Z. PHYSIK.CHEM. N. F.* 1954, **1**, 275.

20. BIRKS, J. B., *CHEM. PHYSICS LETTERS* 1967, 1, 304.

21. FERGUSON, J., *J. CHEM. PHYSICS*, 1962, **37**, 2540.

22. MURRELL, J. N. AND TANAKA, J., *MOLECULAR PHYSICS*, 1964,7,363.

23. CHANDRA, A. K.; LIM, E.C., *J. CHEM. PHYSICS*, 1968, **48**, 2589

24. SHIMADA, K., SZWARC, M. *J. AM. CHEM. SOC.* 1975, **97**, 328

25. FRASER, S., WINNIK, M. *J. CHEM. SOC.* 1981, **75**, 4683

26. HIRAYAMA, F., *J. CHEM. PHYSICS*, 1965, **42**, 3163

27. ZACHARIASS, K.A. AND KUHNLE, W., A. *PHYS. CHEM.(FRANKFURT AM MAIN)* 1976, **101**, 26

28. PERICO, A. AND CUNIBERTI, C., *EUR. POLYM. J.*, 1977, **13**, 369

29. A). WINNIK, M.A., *ACC. CHEM. RES.* 1973, **10**, 1977 B). SNNENSCHEIN, M.F. AND WEISS, R.G., J. PHYS. CHEM. 1988, **92**, 6828 C). ZACHARIASSE, K. AND KUHNLE, W., *Z. PHYS. CHEM.(NEUE FOLGE)* 1976, **10**, 267

30. EATON, F. D; SMART, B. E. *J. AM. CHEM. SOC.*, **1990**, *112*, 2821.

31. HASEK, W.R., SIMTH, W.C., ENGELHARDT, V.A. *J. AM. CHEM. SOC.*, 1960, **82**, 543

32. A) TIERS, G.V.D., *J. AM. CHEM. SOC.*, 1960, **82**, 5513 B)HUYSER, E. S., BEDARD, E., *J. ORG. CHEM.*, 1964, **29**, 1588 C)COWELL, A.B., TAMBORSHI, C., *J. FLUORINE CHEM.*, 1981, 17, 345

33. BRACE, N.O., U.S. PAT. 3,271,441 CA, (1981) 66, 2388Y

34. COE, P.L., MILNER, N.E., *J. FLUORINE CHEM.*,1972/73, **2**, 167

35. WIEDENFELD, D., NIYOGI, S., CHAKRABARTI, D., *J. FLUO. CHEM.*, 2000, **104**, 306

36. BREL, V.K., UVAROV, V.I., ZEFIROV, N.S., STANG, P.S., CAPLE, R., *J. ORG. CHEM.*, 1993, **58**, 6922

37. FURNISS, B. S., HANNAFORD, A. J. *VOGEL'S TEXTBOOK OF PRACTICAL ORGANIC CHEMISTRY*; PP 426, FIFTH EDITION, LONGMAN SCIENTIFIC AND TECHNICAL PUBLISH

38. LAU, C.K., *J. ORG. CHEM.* 1986, **51**, 3038

39. GRUTTNER, G. AND KRAUS, E., *BERICHTE DER DEUTSCHEN CHEAMISCHEN GESELLSCHAFT*, 1916, **49**, 437